Understanding the acid behavior of zeolites from theory and experiment

resulting in the erroneous conclusion that the liquid was nonvolatile.

Our results also bring into question whether the spreading is mainly from flow or diffusive processes as previously assumed[5,8–10]. We have found that if an initially clean wafer is placed several millimetres away from a TEHOS-coated wafer in the same Petri dish, the clean wafer will develop a 5-Å-thick film over a few weeks, by readsorbing TEHOS that has evaporated from the coated wafer. This result indicates the importance of evaporation and readsorption to the spreading of TEHOS, recently also shown to be the dominant spreading mechanism for droplets of moderately volatile liquids[13]. An unresolved question is whether molecular layering can occur in other types of liquid films solely by flow, as originally suggested[4]. By experimenting with liquids whose volatility relative to their ability to flow is much lower than that of TEHOS, it should be possible to distinguish between evaporation and flow mechanisms in the molecular layering. □

Received 13 October 1992; accepted 20 April 1993.

1. Cazabat, A. M., Fraysse, N., Heslot, F. & Carles, P. *J. phys. Chem.* **94**, 7581–7585 (1990).
2. Heslot, F., Fraysse, N. & Cazabat, A. M. *Nature* **338**, 640–642 (1989).
3. Heslot, F., Cazabat, A. M. & Levinson, P. *Phys. Rev. Lett.* **62**, 1286–1289 (1989).
4. Heslot, F., Cazabat, A. M.; Levinson, P. & Fraysse, N. *Phys. Rev. Lett.* **65**, 599–602 (1990).
5. Cazabat, A. M., Heslot, F. & Fraysse, N. *Prog. Colloid Polymer Sci.* **83**, 52–55 (1990).
6. Prenzlow, C. F. & Halsey, G. D. Jr *J. phys. Chem.* **61**, 1158–1165 (1957).
7. Hillner, P. E., Manne, S., Gratz, A. J. & Hansma, P. K. *Ultramicroscopy* **42–44**, 1387–1393 (1992).
8. De Gennes, P. G. & Cazabat, A. M. *C.R. Acad. Sci. Paris, Ser. II* **310**, 1601–1606 (1990).
9. Fraysse, N., Cazabat, M. & Cazabat, A. M. *C.R. Acad. Sci. Paris, Ser. II* **314**, 1025–1028 (1992).
10. Nieminen, J. A., Abraham. D. B., Karttunen, M. & Kaski, M. *Phys. Rev. Lett.* **69**, 124–127 (1992).
11. Yang, J.-x., Koplik, J. & Banavar, J. R. *Phys. Rev. Lett.* **67**, 3539–3542 (1991).
12. Yang, J.-x., Koplik, J. & Banavar, J. R. *Phys. Rev.* A**46**, 7738–7749 (1992).
13. Novotny, V. J. & Marmur, A. *J. Colloid Interf. Sci.* **145**, 355–361 (1991).

ACKNOWLEDGEMENTS. We thank G. Vurens, A. Homola, V. Novotny and C. Gudeman for useful discussions, and the Ministry of Education and Science of Spain and the Fulbright Commission in the U.S. for post-doctoral support for M.L.F.

Understanding the acid behaviour of zeolites from theory and experiment

G. J. Kramer, R. A. van Santen, C. A. Emeis & A. K. Nowak

Koninklijke/Shell-Laboratorium, Amsterdam, (Shell Research B. V.), PO Box 3003, 1003 AA Amsterdam, The Netherlands

ZEOLITES are microporous aluminosilicates which, in their protonated form, act as solid catalysts[1], and are widely used in the oil and petrochemical industries for processes such as cracking, isomerization and alkylation if hydrocarbons[2]. The proposed mechanisms[3–5] of these processes mostly involve proton transfer and formation of carbenium or carbonium ions as reactive intermediates, but the detailed function of the zeolite and in particular the relation between acidity and catalytic activity is not well understood. Here we report experimental and theoretical studies of denterium–hydrogen exchange between deuterated methane and protonated zeolites — a prototypical heterogeneous catalytic reaction between a hydrocarbon and an acid zeolite. We monitored this slow exchange reaction in two different zeolites using infrared spectroscopy, and used *ab initio* quantum chemistry calculations to determine both the reaction mechanism and the acidity–activity relationship. Combining our theoretical results with recent estimates[8–11] of the acidity differences within zeolites enables us to reproduce the experimentally observed reaction rates and thus to obtain a detailed microscopic picture of this heterogeneous catalytic process.

The isotope exchange reaction was monitored by measuring the evolution of the infrared absorption spectrum of a zeolite disk in a closed container in contact with an excess of deuteromethane. Two zeolite samples were used, one with the faujasite (FAU) structure (Si:Al ratio = 10), the other having the ZSM-5 (or MFI) structure (Si:Al ratio = 13). Over time, we observed the disappearance of the absorption bands corresponding to the OH stretch vibration of acid Al–O(H)–Si and terminal SiOH (silanol) groups, with the simultaneous appearance of the corresponding OD and SiOD bands. A control experiment with the pure-silica form of MFI, which contains no acid OH groups, showed that silanol groups are not active in the exchange process. The simultaneous replacement of silanol and acid hydrogen by deuterium in the acid zeolites should be attributed to the intra–zeolite exchange of hydrogen, possibly assisted by trace amounts of water, which is rapid compared with the D/H exchange between the zeolite and deuteromethane[6,7]. The rate of conversion of acid OH groups was measured at temperatures between 620 and 750 K for a methane gas pressure of 13 torr. The lower temperature limit was dictated by the low reaction rate and the upper limit by the onset of methane pyrolysis. The experimental exchange rates (Fig. 1) show a clear difference in activity between FAU and MFI.

We will now turn to first-principles calculation of the results. We apply quantum chemistry to a molecular system in which the zeolite is represented by a molecular cluster. The exchange process is influenced in real zeolites by the variation of proton affinity between crystallographically different oxygen sites. For FAU and MFI, these differences have been quantified[8–11]. We will show that proton affinity differences alter that rate of exchange enough to account for the observed activity difference between zeolites FAU and MFI.

The molecular system used in the *ab initio* quantum chemical study consisted of methane and a tri-tetrahedral SiH_3–OH–$Al(OH)_2$–O–SiH_3 cluster representing the acid zeolite. The peripheral bonds of the cluster, which are in reality connected to the zeolite framework, were saturated with hydrogen atoms. Because of the flexibility of the zeolite lattice, such a cluster is a good model system for the extended

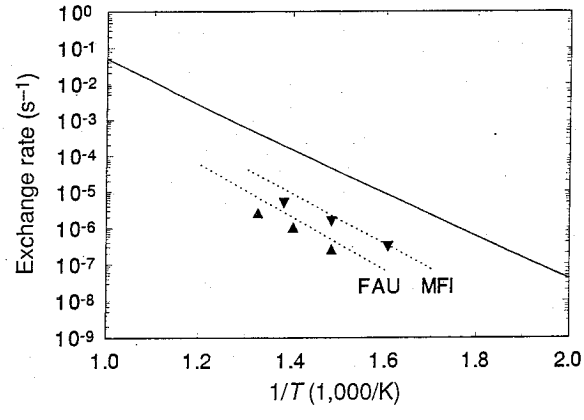

FIG. 1 D/H exchange rate of deuterated methane with the H-forms of zeolites FAU and MFI. Experimental values are given by the full symbols (FAU ▲, MFI ▼). The full line is the prediction from transition-state theory for the exchange reaction with a zeolite cluster, which has an effective reaction barrier of 122 kJ mol^{-1}. Proton affinity differences reduce the exchange rate in real zeolites. The theoretical predictions for zeolites FAU and MFI are indicated by dashed lines.

zeolite[12,13]. Both the adsorption minimum of methane and the transition state for D/H exchange were found using standard conjugate-gradient geometry-optimization methods[14]. The energy difference between the adsorption minimum and transition state for self-consistent-field (SCF) calculations[15] is 180 kJ mol^{-1} when using a 3-21G basis and 230 kJ mol^{-1} with a larger 6-31G** basis. Additional single–double configuration interaction calculations including Pople size-consistency corrections[15] allowed for the estimation of electron correlation effects which are neglected at the SCF level. Electron correlation reduces the barrier by 40 to 60 kJ mol^{-1}, leading to an estimate of 150 ± 20 kJ mol^{-1} for the barrier. Figure 2 shows the calculated transition state and the reaction coordinate.

The reaction coordinate represents the transfer of the proton of the zeolite to the methane molecule and the symmetrical return of one of the deuterium atoms to the zeolite. Thus, the exchange process uses two of the oxygen atoms of the zeolite: one as an acid, the other as a base. In the transition state the exchanging atoms are halfway between the oxygen and carbon atoms, at distances of 1.201 and 1.391 Å, respectively. These short distances indicate that, in the transition state, the hydrocarbon fragment is covalently bonded to the zeolite lattice.

Once the barrier height and the results of the vibrational analysis of initial state and transition state are known, the exchange rate can be theoretically predicted using Eyring's transition state theory[16]. This approach has been successfully applied for simple gas-phase reactions[17,18]. As measurements were made under constant pressure, the reference value for the (free) energy is that of the gas phase. Hence the effective, experimental barrier, on which the exchange rate depends exponentially, is equal to the barrier as calculated from the cluster calculations, corrected by the adsorption energy of methane in the zeolite at zero temperature, which is ~ -28 kJ mol^{-1} for both FAU and MFI[19–21]. The pre-exponential factor depends on the entropy change between the initial state and the transition state, determined by the respective vibrational frequencies. Quantum corrections[22] turned out to be of minor importance. The resulting prediction is shown in Fig. 1, represented by a solid line.

So far we have treated the exchange process as if the zeolite were a molecular catalyst. In doing so, we have neglected the variation of acidity within the zeolite lattice. Recent theoretical studies[8,11] using classical force-field methods, have estimated these differences in zeolites FAU and MFI to be as large as 60 kJ mol^{-1}. The exchange rate obviously changes substantially if proton affinity differences affect the exchange barrier.

We established the relation between acidity and catalytic activity for the D/H exchange reaction through a series of quantum-chemical cluster calculations in which the peripheral SiH bonds of the cluster were fixed at varying distances. As a result, the strength of the SiO bond, and thereby the strength of the acid OH bond, could be strengthened or weakened at will. On changing the SiH distances of one of the peripheral SiH_3 groups between 1.3 and 1.7 Å, the proton affinity of the associated oxygen atom varied by $\sim$ 60 kJ mol^{-1}, thereby mimicking the acidity variation in real zeolites.

Two series of calculations were done. First, the SiH distances in the two SiH_3 groups were varied jointly. Thus, the proton binding strength (acidity) of both oxygen atoms involved in the exchange process remained equal. The barrier height was unaffected, which is explained by the covalent character of the transition state in which the OH bond strength of the initial state is shared between two partial OH bonds (Fig. 2). Second, we simulated the effect of acidity differences by lowering the proton affinity of the proton-accepting oxygen site only. In this case, again because of the covalent bond-sharing character of the transition state, the barrier was increased, proportional to the difference in proton affinity between donor and acceptor site (with constant of proportionality 0.7). In summary, the covalent character of the exchange process enforces a non classical relationship between acidity and activity, where activity is determined by acidity differences between the proton donating and accepting oxygen sites.

As the reaction rate is the product of occupation by protons of a given oxygen site and the probability of exchange from that site, it is always adversely affected by proton affinity differences. Therefore the exchange rate found for the molecular catalyst, where proton affinities are equal, is predicted to be the upper limit for the exchange rate in any aluminosilicate material.

Having established the relation between proton affinity differences and the rate of D/H exchange, we may use the proton affinity data for FAU and MFI from ref. 11 to calculate the reduction of the exchange rate in these zeolites. For both zeolites all T-sites which are the sites that can be occupied by aluminium, were considered. For each of these there are six possible exchange paths between any of the four oxygen atoms surrounding the central aluminium. Some paths are sterically inaccessible: in zeolite FAU, for instance, there is a unique crystallographic T-site[23] surrounded by four difference oxygen

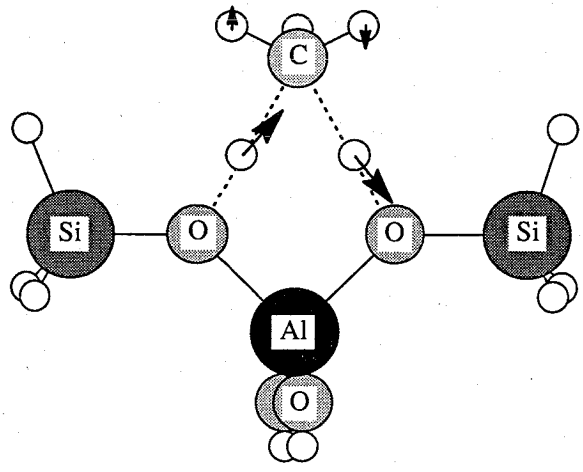

FIG. 2 Calculated transition-state geometry for the isotope exchange process between methane and an acid zeolite cluster. All small circles represent hydrogen or deuterium atoms. The arrows indicate the main components of the displacement vectors along the reaction coordinate.

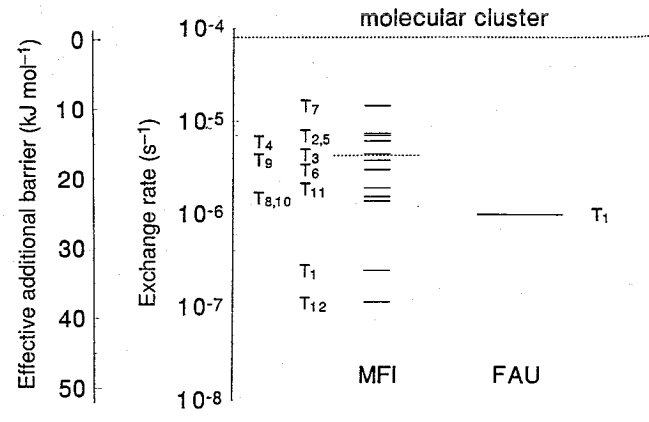

FIG. 3 Site-dependent exchange rates in zeolites FAU and MFI at 700 K and 13 torr methane pressure. These zeolites have a lower exchange rate than the molecular catalyst, because a higher effective barrier is induced by proton affinity differences between the oxygen sites. The dashed line indicates the average exchange rate for MFI. The numbering of T-sites in zeolite MFI is taken from ref. 23; FAU has one unique T-site.

sites, one of which does not take part in the exchange process because a proton on this site protrudes into the sodalite cage, which is inaccessible to methane. For the remaining three accessible pathways, the proton affinity differences are 35 kJ mol^{-1} or higher. In combination with the appropriate Boltzmann factors for the proton occupancy of oxygen sites, this leads to a reduction of the exchange rate by a factor of 80 at 700 K compared with the molecular catalyst.

MFI has a more complex crystal structure with 12 different T-sites[23]. For each of these, we repeated the calculation outlined above. Between different T-sites, the exchange rate varied by two orders of magnitude (Fig. 3). The large activity differences corroborate empirical evidence that the acid sites are heterogeneous[24]. Assuming a random distribution of aluminium over all T-sites, the overall exchange rate in MFI is the average of these exchange rates, which at 700 K is a factor of 20 lower than that of the molecular catalyst and thus a factor 4 larger than in FAU. These reduction factors vary with temperature; the predicted reaction-rate dependencies are shown by dashed lines in Fig. 1.

The theoretical predictions of the relative rates for the two zeolites and their temperature dependence agree well with experiment. It should be mentioned that there is a 20 kJ mol^{-1} uncertainty in the absolute value of the barrier as predicted by quantum chemistry. But this uncertainty affects the predictions for all zeolites to the same extent, so the prediction of a factor of four difference in reactivity between zeolites FAU and MFI is not affected.

Our results show that heterogeneous catalysts can be understood at the atomic level, and that quantitative agreement between theory and experiment can be achieved. For the exchange reaction studied here, we have predicted the reaction path and established the relationship between acidity and catalytic activity. When combined with theoretical estimates for the proton affinity of the various oxygen sites within the zeolite, this gives an *ab initio* prediction of heterogeneous catalytic activity. Applying the argument in reverse, it gives a first, albeit indirect, experimental measure of the acidity differences in zeolites, which must be ~ 60 kJ mol^{-1} to explain satisfactorily the reactivity differences between FAU and MFI. □

Received 29 January; accepted 7 May 1993.

1. Thomas, J. M. *Scient. Am.*, **266** (IV), 82–88 (1992).
2. Maxwell, I. E. & Stork, W. H. J. in *Introduction to Zeolite Science and Practice*, (eds van Bekkum, H. *et al.*) 571–630 (Elsevier, Amsterdam, 1991).
3. Jacobs, P. A. & Martens, J. A. in *Introduction to Zeolite Science and Practice*, (eds van Bekkum, H. *et al.*) 445–496 (Elsevier, Amsterdam, 1991).
4. Abbot, J. & Wojciechowski, B. W. *J. Catal.* **115**, 1–15 (1989).
5. Stefanidis, C., Gates, B. C. & Haag, W. O. *J. Molec. Catal.* **67**, 363–367 (1991).
6. Sauer, J., Kölmel, C. M., Hill, J. R. & Ahlrichs, R. *Chem. Phys. Lett.* **164**, 193–198 (1989).
7. Sauer, J., Horn, H., Häser, M. & Ahlrichs, R. *Chem. Phys. Lett.* **173**, 26–32 (1990).
8. Dubsky, J. Beran, S. & Bosáček, V. *J. Molec. Catal.* **6**, 321–326 (1979).
9. Schröder, K.-P., Sauer, J., Leslie, M., Catlow, R. C. A. & Thomas, J. M. *Chem. Phys. Lett.* **188**, 320–325 (1992).
10. Schröder, K.-P., Sauer, J., Leslie, M. & Catlow, R. C. A. *Zeolites* **12**, 20–23 (1992).
11. Kramer, G. J. & van Santen, R. A. *J. Am. chem. Soc.* **115**, 2887–2897 (1993).
12. Kramer, G. J., de Man, A. J. M. & van Santen, R. A. *J. Am. chem. Soc.* **113**, 6435–6441 (1991).
13. Sauer, J. *chem. Rev.* **89**, 199–255 (1989).
14. Dupuis, M., Sprangler, D. & Wendolowski, D. *NRCC Software Catalog 1*, Program No. QG01, GAMESS (1980).
15. Szabo, A. & Ostlund, N. S. *Modern Quantum Chemistry: Introduction to Advanced Electronic Structure Theory* (Macmillan, New York, 1982).
16. Rice, O. K. *Statistical Mechanics, Thermodynamics and Kinetics* (Freeman, San Francisco, 1966).
17. Thruhlar, D. G. & Gordon, M. S. *Science* **249**, 491–497 (1990).
18. Gilbert, R. G. & Smith, S. C. *Theory of Unimolecular and Recombination Reactions* (Blackwell, Oxford, 1990).
19. Barrer, R. M., & Sutherland, J. W. *Proc. R. Soc.* **A237**, 439–450 (1956).
20. Papp, H., Hinsen, W., Do, N. T. & Baerns, M., *Thermochim. Acta* **82**, 137–148 (1984).
21. Yashonath, S., Thomas, J. M., Nowak, A. K. & Cheetham, A. K. *Nature* **331**, 601–604 (1988).
22. Johnston, H. S. *Gas Phase Reaction Rate Theory* (Ronald, New York, 1966).
23. Meier, W. M. & Olson, D. H. *Atlas of Zeolite Structure Types*, 2nd edn (Butterworth, Cambridge, 1987).
24. Lombardo, E. A., Sill, G. A. & Hall, W. K. *J. Catal.* **119**, 426–440 (1989).

ACKNOWLEDGEMENTS: We thank B. J. Milan for help in the experimental work.

Milankovitch theory viewed from Devils Hole

J.Imbrie*, A. C. Mix† & D. G. Martinson‡

*Department of Geological Sciences, Brown University, Providence, Rhode Island 02912, USA
†College of Oceanography, Oregon State University, Corvallis, Oregon, 97331, USA
‡Lamont-Doherty Earth Observatory of Columbia University, Palisades, New York 10964, USA

VARIATIONS in the oxygen isotope content ($\delta^{18}O$) of late Quaternary deep-sea sediments mainly reflect changes in continental ice mass[1], and hence provide important information about the timing of past ice ages. Because these sediments cannot yet be dated directly beyond the range of radiocarbon dating (40-50 kyr), ages for the $\delta^{18}O$ record have been generated[2,3] by matching the phase of the changes in $\delta^{18}O$ to that of variations in the Earth's precession and obliquity. Adopting this timescale yields a close correspondence between the time-varying amplitudes of these orbital variations and those of a wide range of climate proxies[4], lending support to the Milankovitch theory that the Earth's glacial-interglacial cycles are driven by orbital variations. Recently Winograd *et al.*[5] reported a record of $\delta^{18}O$ variations in a fresh-water carbonate sequence from Devils Hole, Nevada, dated by U–Th disequilibrium[6]. They concluded that the timing of several of the features in the record, which reflects changes in the temperature of precipitation over Nevada as well as changes in the isotopic composition of the moisture source[5,7], showed significant deviations from that predicted by Milankovitch theory. Here we demonstrate that applying the Devils Hole chronology to ocean cores requires physically implausible changes in sedimentation rate. Moreover, spectral analysis of the Devils Hole record shows clear evidence of orbital influence. We therefore conclude that transfer of the Devils Hole chronology to the marine record is inappropriate, and that the evidence in favour of Milankovitch theory remains strong.

The Devils Hole $\delta^{18}O$ record was obtained from a 36-cm core (DH-11) drilled in a layer of calcite lining a water-filled cavern in southern Nevada. Ground water here originates as snow and rain in the surrounding mountains[5]. The time resolution of the $\delta^{18}O$ record is comparable to that in deep-sea records and contains 21 precise radiometric dates[6] from the ^{230}Th method[8]. The general resemblance of the Devils Hole $\delta^{18}O$ record to that of the ocean is striking (Fig. 1). Indeed, the coherency is so high that it is tempting to overlook how different the physics underlying each record must be and jump to the conclusion that they are in fact synchronous. The SPECMAP marine $\delta^{18}O$ stack is an average of many open-ocean records in which values become heavier during glacial intervals, mainly because of storage of fresh water as ice. In contrast, the $\delta^{18}O$ data in DH-11 reflect the isotopic distillation of atmospheric moisture, a process linked to local precipitation temperature[5]. Values in this record therefore become lighter during glacial intervals. But to interpret these data properly as an air temperature signal, one must make assumptions not only about the isotopic composition of the oceanic moisture source (which changes over a glacial cycle), but also about air-parcel trajectories at the relevant seasons[7]. Winograd *et al.*[5] address some, but not all, of these complex issues.

A convenient way of comparing the DH-11 and SPECMAP chronologies is to examine a mapping function[9] that adjusts the ages in one curve to give the best match with $\delta^{18}O$ variations in the other (Fig. 2). Overall, the similarity between these physically very different records is remarkable (r=0.85). But we focus here on two glacial intervals, stages 6 and 10, in which the DH-11 ages are significantly older.